

# RESEARCH ON AERODYNAMIC NOISE CHARACTERISTICS OF HELICOPTER ROTORS CONSIDERING THE INFLUENCE OF BLADE SHAPES

Quang Quyen Le<sup>1,\*</sup>, Thanh Dong Pham<sup>1</sup>, Quoc Tru Vu<sup>1</sup>, Anh Tuan Nguyen<sup>1</sup>

<sup>1</sup>*Faculty of Aerospace Engineering, Le Quy Don Technical University, Hanoi, Vietnam*

## Abstract

In this study, we investigated the influence of blade shapes on the aerodynamic noise characteristics of helicopter main rotors by the vortex method. The obtained results are the variation of the time-dependent lift coefficient of rotors and the aerodynamic noise characteristics of the helicopter rotor with different blade shapes. On that basis, the influence of the blade shape on the aerodynamic noise characteristics of helicopter rotors was evaluated. An advanced blade shape was designed to reduce the aerodynamic noise of rotors while maintaining the lift of the rotor. Computational results show that the rotor with the advanced blade generates the lower noise, and the noise of the advanced blade reduces by up to 6.15 dB (reduced by 6.90%) compared with the common rectangular blade in hover and up to 5.4 dB (reduced by 5.15%) in forward flight.

**Keywords:** *Vortex method; helicopter main rotors; rotor blade shapes; aerodynamic noise.*

## 1. Introduction

Helicopters often generate loud noise during operations, causing serious noise pollution. Sources of the aerodynamic noise on helicopters include the engine noise, transmission noise, main rotor noise, tail rotor noise, main rotor - tail rotor interaction noise. In particular, the helicopter main rotor is the component that causes the largest aerodynamic noise. Hence, researching the reduction of the aerodynamic noise of helicopter rotors is becoming a great necessity and has a very important meaning. Therefore, more and more researchers have carried out research on the optimization design of noise reduction for helicopter rotors.

There were many kinds of research on the aerodynamic noise of helicopter rotors, and most of them used the Ffowcs Williams-Hawkings (FW-H) equation [1-3] to describe the noise generation caused by the motion of rotors in the turbulent flow. Many researchers used the CFD simulation method to predict the noise of rotors based on solving RANS equations [4-6]. Other investigators used experimental methods, such as wind tunnels and testing flight to measure the aerodynamic noise [7-9]. N.H. Son [10]

---

\* Email: le.quang-quyen@lqdtu.edu.vn  
DOI: 10.56651/lqdtu.jst.v18.n03.613

used the CFD method on Ansys Fluent software to research the aerodynamic noise of helicopter rotors.

In the present work, we investigate the influence of blade shapes on the aerodynamic noise characteristics of helicopter rotors by using the vortex method. In which, we first focus on studying the effect of the blade tip shape on the "thickness noise" component and the sound pressure level (SPL) generated by the helicopter main rotor. Then, carry out a design of an advanced blade for reducing the aerodynamic noise of the helicopter main rotor.

## 2. Methodology

To determine the aerodynamic noise characteristics of rotors, it is necessary to solve two main problems: the aerodynamic problem and the aerodynamic noise problem. In which the pressure distribution calculated from the aerodynamic problem act as input parameters and the noise source of the aerodynamic noise problem.

The aerodynamic problem determines the aerodynamic characteristics of the rotor and the pressure distribution on the rotor surface. For this problem, we use the vortex method to build a model of rotors and calculate the aerodynamic characteristics of rotors, determine the pressure distribution on the rotor surface, and simulate the vortex wake generated behind the rotor. The contents of model building, setting boundary conditions, and calculating and verifying results of aerodynamic problems are presented in detail in the works [11-13].

The aerodynamic noise problem determines the aerodynamic noise characteristics of the rotor based on the Ffowcs Williams-Hawkings (FW-H) equation. In which, pressure distributions calculated from the aerodynamic problem are input parameters - the source of the aerodynamic noise in the aerodynamic noise problem.

Ffowcs Williams-Hawkings studied the aerodynamic noise generation by turbulent flows and the lifting surface moving in turbulent flows and constructed the FW-H equation to determine the acoustic pressure and its propagation in the air. The sound pressure can be determined using Formulations 1 and 1A of Farassat et al. [2], which is one of the solutions of the FW-H equation. These formulations assumed the propagation of sound waves in a stationary medium.

Formulation 1A of Farassat [2] is given by:

$$p'(x,t) = p'_T(x,t) + p'_L(x,t) \quad (1)$$

where  $p'(x,t)$  is the total acoustic pressure at observers;  $p'_T(x,t)$  and  $p'_L(x,t)$  are the pressure causing thickness noise and loading noise, respectively, and can be written as:

$$p'_T(x,t) = \frac{1}{4\pi} \int_{f=0} \left[ \frac{\rho_0 \dot{v}_n}{r(1-M_r)^2} + \frac{\rho_0 v_n \hat{r}_1 \dot{M}_1}{r(1-M_r)^3} \right]_{ret} dS + \frac{1}{4\pi} \int_{f=0} \left[ \frac{\rho_0 c v_n (M_r - M^2)}{r^2 (1-M_r)^3} \right]_{ret} dS \quad (2)$$

$$p'_L(x,t) = \frac{1}{4\pi c} \int_{f=0} \left[ \frac{\dot{p} \cos(\theta)}{r(1-M_r)^2} + \frac{p \cos(\theta) \hat{r}_1 \dot{M}_1}{r(1-M_r)^3} \right]_{ret} dS + \frac{1}{4\pi} \int_{f=0} \left[ \frac{p(\cos(\theta) - M_r n_i)}{r^2 (1-M_r)^2} + \frac{p \cos(\theta) (M_r - M^2)}{r^2 (1-M_r)^3} \right]_{ret} dS \quad (3)$$

where  $[\dots]_{ret}$  denotes the evaluation at the retarded time

$$\tau = t - \frac{r}{c} = t - \frac{|\mathbf{x} - \mathbf{y}|}{c} \quad (4)$$

where  $p$  is the pressure at source points;  $c$  is the speed of sound;  $\rho_0$  is the airflow density;  $t$  is the time at observers;  $\tau$  is the retarded time when the noise is emitted from the source to the observer;  $r = |\mathbf{x} - \mathbf{y}|$  is the distance between the observer and the source,  $\mathbf{x}$  is the observer position vector,  $\mathbf{y}$  is the source position vector.  $M_r = \dot{M}_1 \hat{r}_1$  is the Mach number of source in radiation direction;  $v_n$  is the local normal velocity to blade surface; the subscripts  $n$  and  $r$  represent terms in the normal and emission directions with the blade surface;  $f = 0$  is a function describing the blade surface (source surface);  $\cos(\theta) = \mathbf{n} \cdot \hat{\mathbf{r}}$  with  $\theta$  used to denote the angle between the normal vector  $\mathbf{n}$  to the emission surface and the radiation direction  $\mathbf{r}$  at the time of emission [2, 13].

In the present work, we use the Formulation 1C of Najafi et al. [3] to determine the sound pressure generated by the rotor. The Formulation 1C of Najafi is a surface integral formulation based on the convective wave equation, which takes into account the presence of mean flow. This formulation is an extension of Farassat's Formulations 1 and 1A based on the convective form of the FW-H equation.

Formulation 1C of Najafi [3] is given by:

$$p'(x,t) = p'_T(x,t) + p'_L(x,t) \quad (5)$$

$$p'_T(x,t) = \frac{1}{4\pi} \frac{\partial}{\partial t} \int_{f=0} \left[ \frac{Q_j n_j}{R^* (1-M_R)} \right]_{ret} dS - \frac{1}{4\pi} M_0 \frac{\partial}{\partial t} \int_{f=0} \left[ \frac{\tilde{R}_1 Q_j n_j}{R^* (1-M_R)} \right]_{ret} dS - \frac{1}{4\pi} U_0 \int_{f=0} \left[ \frac{\tilde{R}_1^* Q_j n_j}{R^{*2} (1-M_R)} \right]_{ret} dS \quad (6)$$

$$p'_L(x,t) = \frac{1}{4\pi c} \frac{\partial}{\partial t} \int_{f=0} \left[ \frac{L_{ij} n_j \tilde{R}_i}{R^* (1-M_R)} \right]_{ret} dS + \frac{1}{4\pi} \int_{f=0} \left[ \frac{L_{ij} n_j \tilde{R}_i^*}{R^{*2} (1-M_R)} \right]_{ret} dS \quad (7)$$

Here

$$Q_j = \rho(u_j + U_{0j} - v_j) + \rho_0(v_j - U_{0j}) \quad (8)$$

$$L_{ij} = \rho u_j (u_j + U_{0j} - v_j) + P_{ij} \quad (9)$$

$$P_{ij} = (p - p_0) \delta_{ij} - \sigma_{ij} \quad (10)$$

$$\tau = t - \frac{R}{c} = t - \frac{|\mathbf{x} - \mathbf{y}|}{c} \quad (11)$$

where  $R = |\mathbf{x} - \mathbf{y}|$  is the distance between the observer and the source,  $M_R = \frac{1}{c} v_i \tilde{R}_i$  is the Mach number of the source in radiation direction,  $\tilde{R}_i$  is the radiation vector,  $Q_j$  and  $L_{ij}$  are the thickness tensor and loading tensor, respectively,  $P_{ij}$  is the stress tensor,  $f=0$  is a function describing the blade surface (source surface),  $\sigma_{ij}$  is the viscous stress tensor,  $\delta_{ij}$  is the Kronecker delta,  $U_0$  is the win-tunnel velocity (forward velocity),  $M_0 = U_0 / c$  is the win-tunnel Mach number,  $u_j$  and  $v_j$  are the flow and the surface velocities, respectively.

Based on Najafi's Formulation 1C, we built a tool for calculating the aerodynamic noise characteristics of rotors, calculated and verified with the results of reputable publications. Details on how to build and verify the calculation tool are presented in detail in works [12, 13]. Verified results show that this tool for calculating the aerodynamic noise characteristics of rotors gives accurate and reliable results.

### 3. Results and discussions

#### 3.1. Calculating and investigating for some different blade shapes

Using a calculation tool verified in previous works [12, 13], carry out calculations and investigations of aerodynamic noise characteristics of helicopter rotors with some different blade shapes in hover and forward flight with the velocity  $v = 50$  m/s.

The model of blades with the shape and geometric parameters is given in Fig. 1.

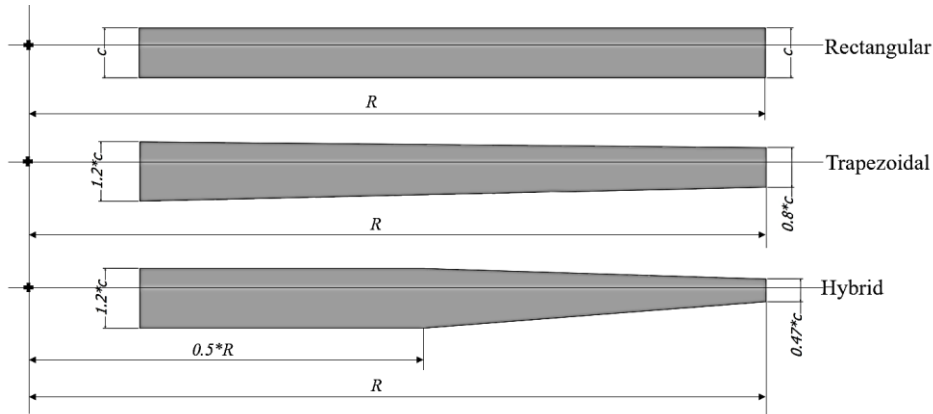


Fig. 1. Model of different rotor blade shapes.

These blades with 3D airfoil NACA0012 are built and meshed on Patran software with geometric parameters as shown in Table 1.

Table 1. Parameters of rotors

| No. | Parameters                           | Rectangular blade | Trapezoidal blade | Hybrid blade      |
|-----|--------------------------------------|-------------------|-------------------|-------------------|
| 1   | Number of blades $n_{blade}$         | 2                 |                   |                   |
| 2   | Rotor radius $R$ , m                 | 1.829             |                   |                   |
| 3   | Rotor rig radius $R_{root}$ , m      | 0.1554            |                   |                   |
| 4   | Blade chord length ( $c = 0.1334$ m) | c                 | $0.8c \div 1.2c$  | $0.47c \div 1.2c$ |
| 6   | Angular speed $\omega$ , rpm         | 1296              |                   |                   |
| 8   | Blade twist, deg                     | 10.9°             |                   |                   |

*a. In hover*

After 800 calculation steps corresponding to 8 revolutions with time steps  $dt = 0.00046296$  s, obtained the variation of the time-dependent lift coefficient of rotors in hover as shown in Fig. 2.

The average lift coefficient value of rotors (rectangular - trapezoidal - hybrid blade) are  $C_L = 0.00287$ ;  $0.00275$  and  $0.00268$ , respectively. From the obtained results, it can be seen that, with the same surface areas of the blade, and the same twist angles, the rotor with the rectangular blade generates a larger lift and the rotor with the hybrid blade generates a smaller lift.

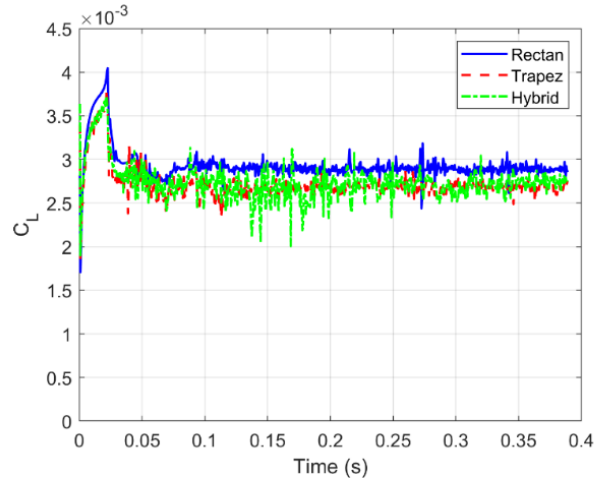


Fig. 2. The variation of the time-dependent lift coefficient of rotors in hover.

From the aerodynamic obtained results, calculating the aerodynamic noise characteristics of rotors at the Microphone 1 with coordinate  $(-1.2R, 0, 0)$  m (Fig. 3).

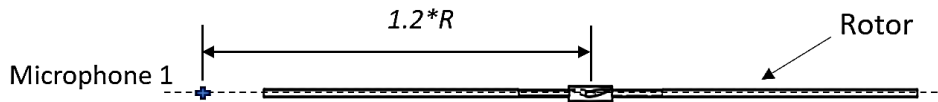


Fig. 3. Microphone position for measuring aerodynamic noise characteristics.

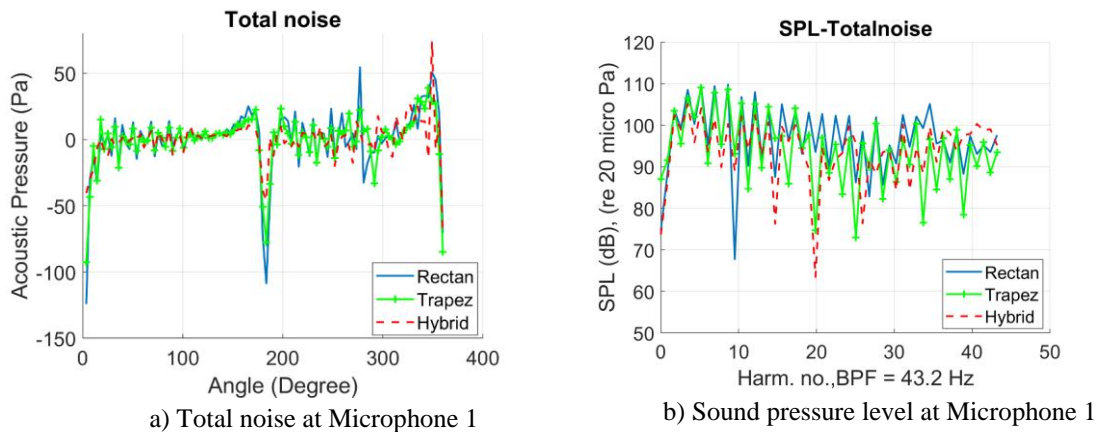


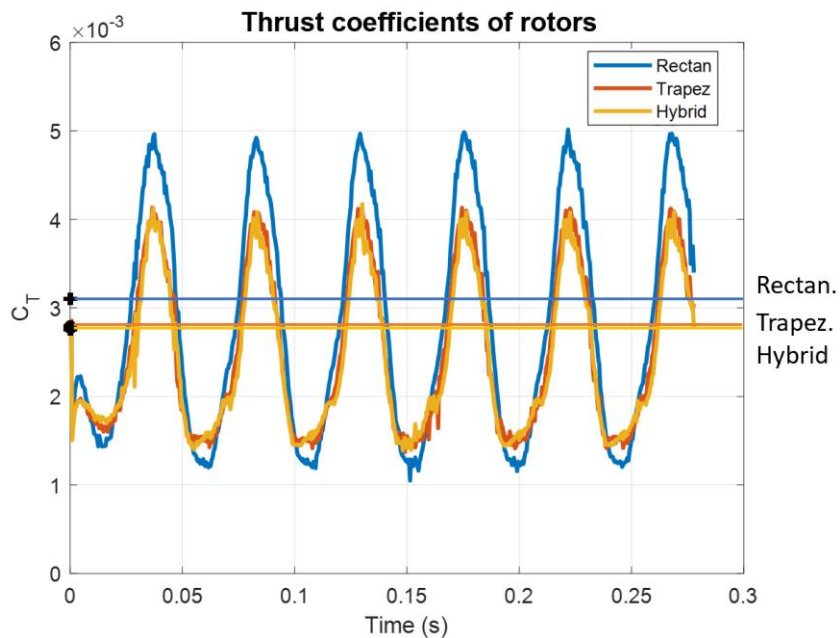
Fig. 4. Comparison of aerodynamic noise characteristics of rotors at Microphone 1 in hover.

Figure 4 (a) shows the comparisons of the acoustic pressure of total noise between the rectangular blade, trapezoidal blade and hybrid blade. It can be seen that, the amplitude of acoustic pressure of the rectangular blade is higher than that of the trapezoidal blade and hybrid blade. The amplitude acoustic pressure of the hybrid blade

is the lowest. Fig. 4 (b) shows the noise comparison results of 3 rotors (rectangular - trapezoidal – hybrid blade). It can be seen that, at low frequency (from 0 to 650 Hz) the hybrid blade generates the lowest noise, and the rectangular blade and trapezoidal blade generate the larger noise. At mid frequency (between 650 and 1050 Hz), the sound pressure level generated by the rectangular blade is the highest. At high frequency (higher 1050 Hz), the sound pressure level generated by 3 blades are almost same.

*b. In the forward flight*

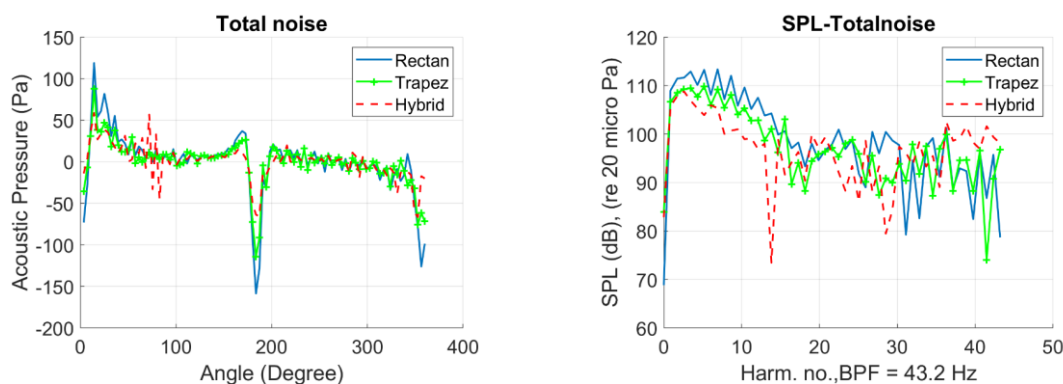
Similarly, carry out calculations of the aerodynamic noise characteristics of helicopter rotors in the forward flight with velocity  $v = 50$  m/s. After 6 revolutions, obtained the variation of the time-dependent thrust coefficient of rotors in the forward flight is shown in Fig. 5.



*Fig. 5. The variation of the time-dependent thrust coefficient of rotors in the forward flight.*

The average thrust coefficient value of rotors (rectangular - trapezoidal - hybrid blade) in the forward flight are  $C_T = 0.003103$ ;  $0.002783$  and  $0.002758$ , respectively. From the obtained results, it can be seen that the same as in hover, the rotor with the rectangular blade generates a larger thrust and the rotor with the trapezoidal blade and the hybrid blade generates a smaller thrust.

From the aerodynamic obtained results, calculating the aerodynamic noise characteristics generated by rotors at the Microphone 1 with coordinate (-1.2R, 0, 0) m, obtained results as shown in Fig. 6.



a) Total noise at Microphone 1

b) Sound pressure level at Microphone 1

Fig. 6. Comparison of the aerodynamic noise characteristics of rotors at Microphone 1 in forward flight.

Figure 6 (a) shows the same results as in hover. The amplitude of acoustic pressure of the rectangular blade is higher than that of the trapezoidal blade and the hybrid blade. And the amplitude of acoustic pressure of the hybrid blade is the lowest. From the obtained results in Fig. 6 (b), it can be seen that, at low frequency (from 0 to 650 Hz) the sound pressure level generates by the rectangular blade is the highest, and the sound pressure level generates by the hybrid blade is the lowest. The peak sound pressure levels generated by 3 blades (rectangular - trapezoidal - hybrid blade) are 113.365 dB, 109.807 dB, and 108.784 dB, respectively. At higher frequency (higher 650 Hz), the sound pressure level generates by 3 blades are almost same.

### 3.2. Designing an advanced blade shape

From the above calculational and investigational results, it can be seen that the rectangular blade generates a larger thrust, the trapezoidal blade and the hybrid blade generate a smaller thrust. Nevertheless, the amplitude of acoustic pressure of the rectangular blade is higher than that of the trapezoidal blade and hybrid blade. The amplitude acoustic pressure of the hybrid blade is the lowest. And at low frequency, the hybrid blade generates the lowest noise, the rectangular blade generates the largest noise. It shows that the blade with a smaller tip generates a lower noise, but the generated lift and thrust are also smaller. Since, we conducted to design an advanced blade shape for maintaining the large lift and thrust while generating the lower noise (Fig. 7).

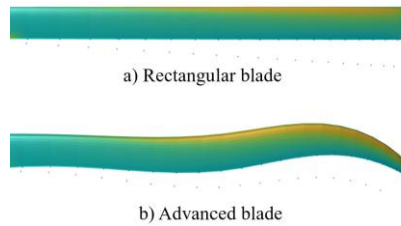


Fig. 7. The pressure distribution on rotor blades.

Compared with the rectangular blade, the advanced blade has a larger twist angle, a larger chord length at the root, and a smaller chord length at the tip. The blade tip has a smaller chord length for reducing the rotor noise. To maintain the large lift and the large thrust, the middle parts of the blade will be designed with larger chord lengths, as shown in Table 2.

Table 2. Parameters of the advanced blade

| No | Parameters                                    | Advanced blade |
|----|-----------------------------------------------|----------------|
| 1  | Airfoil blade                                 | NACA0012       |
| 2  | Rotor radius $R$ , m                          | 1.829          |
| 3  | Root chord length, $c_{root}$                 | 1.1*c          |
| 4  | Chord length at section $0.25R$ , $c_{0.25R}$ | c              |
| 5  | Chord length at section $0.6R$ , $c_{0.5R}$   | 1.12*c         |
| 6  | Chord length at section $0.85R$ , $c_{0.75R}$ | 0.8*c          |
| 7  | Tip chord length $R_{tip}$ , $c_{tip}$        | 0.4*c          |
| 8  | Twist of blades, $\beta$                      | 12°            |

a. In hover

Figure 8 shows the comparison of the lift force between rotors with the rectangular blade and the advanced blade in hover. It can be seen that the average lift forces of these rotors in hover are relatively similar.

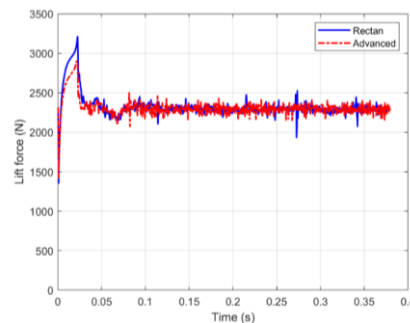


Fig. 8. The variation of the time-dependent lift force of rotors with rectangular blades and with advanced blades in hover.

Conducting calculations of aerodynamic noise characteristics of rotors at positions of Micro. 1 ( $-1.2 \cdot R$ , 0, 0) m, Micro. 2 ( $-1.5 \cdot R$ , 0, 0) m, Micro. 3 ( $-2 \cdot R$ , 0, 0) m, Micro. 4 ( $-3 \cdot R$ , 0, 0) m và Micro. 5 ( $-4 \cdot R$ , 0, 0) m (Fig. 9).

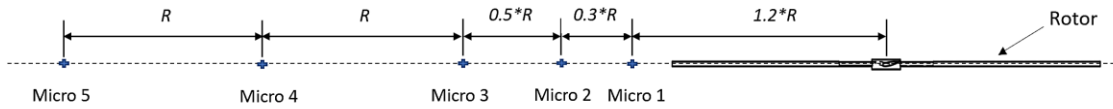


Fig. 9. Microphone positions for measuring aerodynamic noise characteristics.

Figure 10 shows the comparisons of the acoustic pressure variation of thickness noise between the rectangular blade and the advanced blade. It can be seen that, at microphone positions, the amplitude of acoustic pressure of the advanced blade is significantly lower than of the rectangular blade.

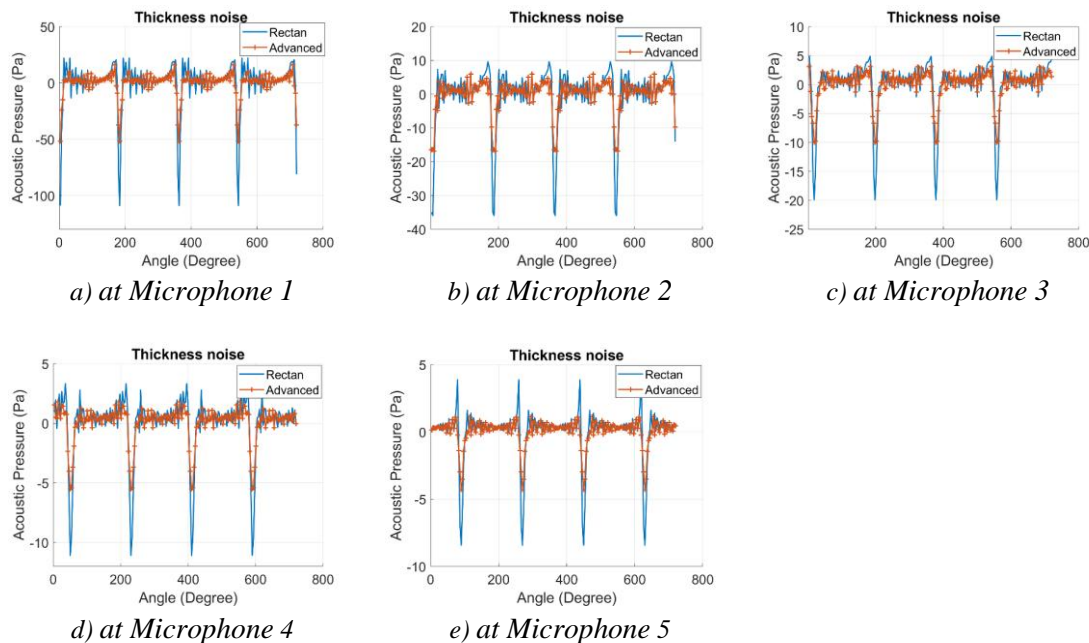


Fig. 10. Comparison of the thickness noise of rotors in hover.

Figure 11 shows the comparisons results of the sound spectra distribution between the rectangular blade and the advanced blade. It can be seen that, at high frequency (higher 850 Hz), the sound pressure level generates by 2 blades are almost same. At low frequency (lower 850 Hz) the sound pressure level generates by the advanced blade is lower than the rectangular blade. The sound pressure level reduction between the advanced blade and the rectangular blade is shown in Table 3.

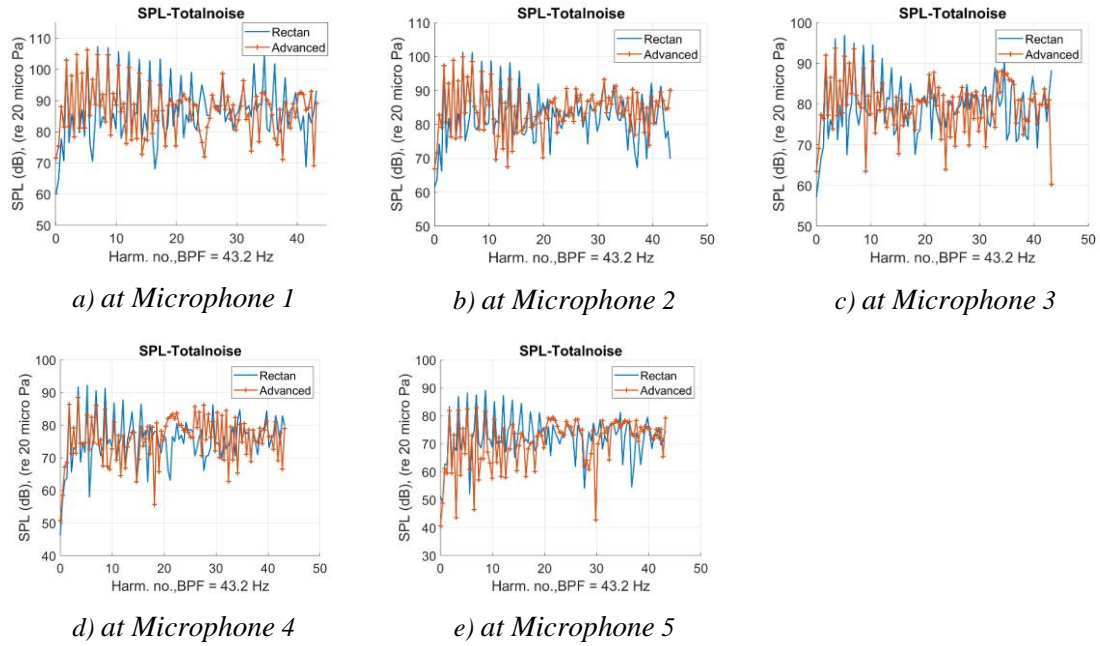


Fig. 11. Comparison of the sound pressure level of rotors in hover.

Table 3. The sound pressure level reduction between the rectangular blade and the advanced blade

| Positions    | SPL peak, dB |          | SPL reduction, dB | SPL reduction |
|--------------|--------------|----------|-------------------|---------------|
|              | Rectangular  | Advanced |                   |               |
| Microphone 1 | 107.298      | 106.26   | 1.038             | 0.97%         |
| Microphone 2 | 101.305      | 99.8869  | 1.4181            | 1.40%         |
| Microphone 3 | 96.8806      | 93.727   | 3.1536            | 3.26%         |
| Microphone 4 | 92.2366      | 88.4958  | 3.7408            | 4.06%         |
| Microphone 5 | 89.1024      | 82.95    | 6.1524            | 6.90%         |

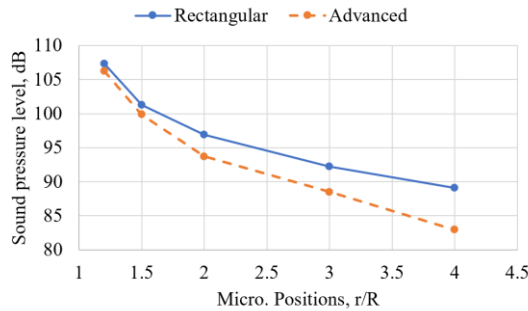


Fig. 12. Comparison of the sound pressure level between the rectangular blade and the advanced blade at the microphone positions.

Figure 12 and Table 3 show that, the further away from the rotor, the sound pressure level of the advanced blade is lower than the sound pressure level of the rectangular blade and can be reduced by up to 6.15 dB (reduced 6.90%) in compared with the sound pressure level of the rectangular blade.

*b. In the forward flight*

Figure 13 shows the variation of the time-dependent thrust of rotors in the forward flight with velocity  $v = 50$  m/s. It can be seen that the thrust values of these rotors in the forward flight are relatively similar.

Perform calculations of aerodynamic noise characteristics of rotors at positions of Micro. 1 ( $-2*R, 0, 0$ ) m and Micro. 2 ( $-2*R, 0, -0.2*R$ ) m (Fig. 14).

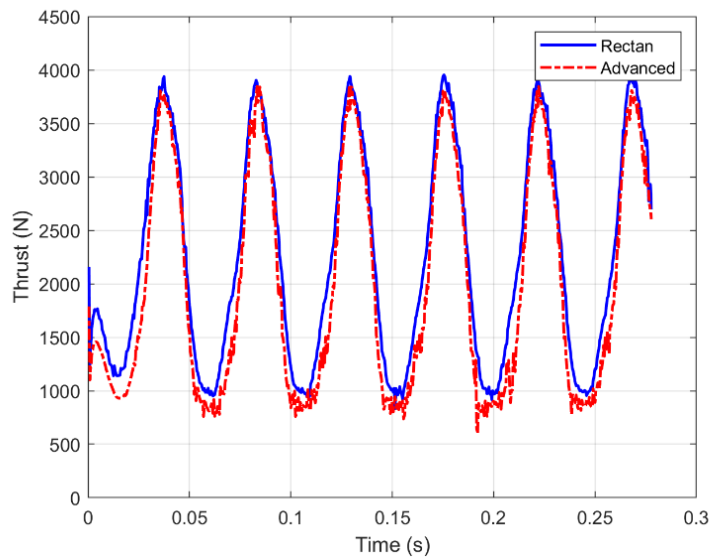


Fig. 13. The variation of the time-dependent thrust of rotors with the rectangular blade and the advanced blade in hover.

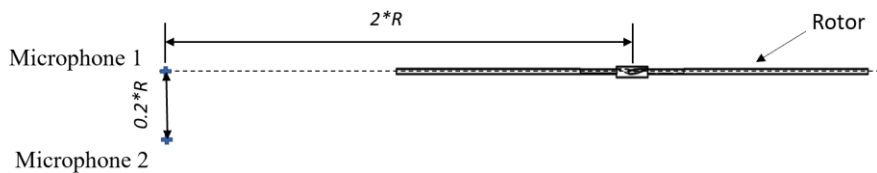


Fig. 14. Microphone positions for measuring aerodynamic noise characteristics.

Figure 15 shows the same results as in hover, at microphone positions, the amplitude of acoustic pressure of the advanced blade is significantly lower than that of the rectangular blade. At high frequency (higher 1200 Hz), the sound pressure level generates by 2 blades are almost same. At low frequency (lower 1200 Hz) the sound

pressure level generates by the advanced blade is lower than by the rectangular blade. The advanced blade can reduce the sound pressure level by up to 5.4 dB (reduced 5.15%) in compared with the rectangular blade.

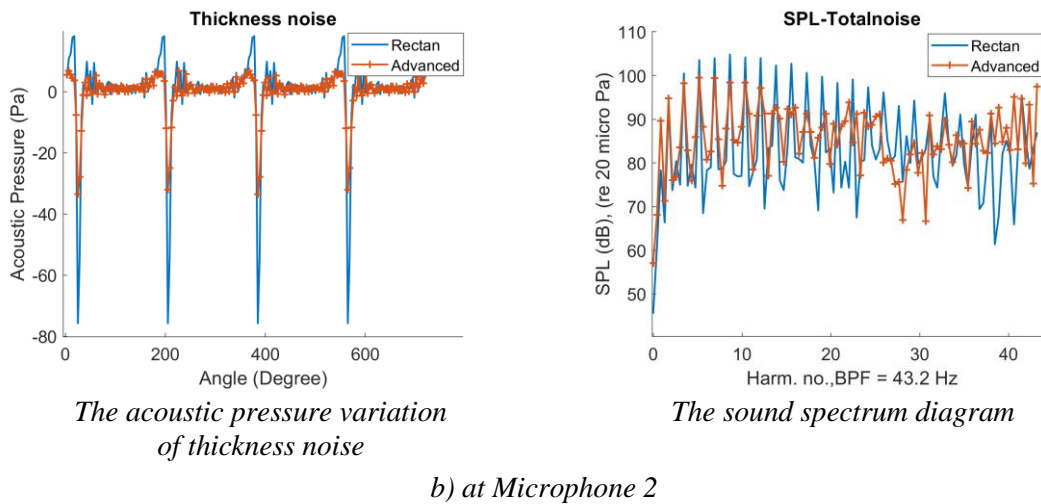
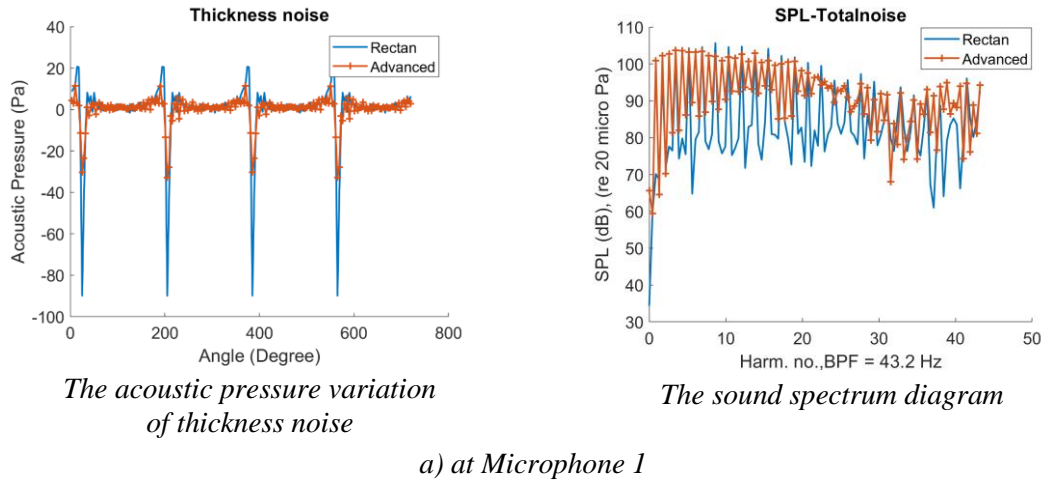


Fig. 15. Comparison of aerodynamic noise characteristics of rotors at Microphone positions in forward flight.

#### 4. Conclusions

In this article, by using a tool for calculating the aerodynamic noise characteristics of helicopter rotors built and verified in previous works, the aerodynamic noise characteristics of helicopter rotors were calculated with different blade shapes (rectangular - trapezoidal - hybrid blade). Obtained results showed that rotors with a smaller blade tip generated a lower noise, but the lift was also smaller and oppositely.

With the aim of conducted an advanced design of the blade shape to reduce the aerodynamic noise of the rotor while still maintaining the large lift, calculational results

showed that at low frequency, the sound pressure level of the advanced blade was lower than that of the rectangular blade. The further away from the rotor, the sound pressure level of the advanced blade is lower than that of the rectangular blade.

It can be seen that, in hover, the sound pressure level of the advanced blade can be reduced by up to 6.15 dB (reduced 6.90%) in compared with the sound pressure level of the rectangular blade. And, in forward flight, it can be reduced by up to 5.4 dB (reduced 5.15%).

## References

- [1] Ffowcs Williams J. and Hawkins D., “Sound Generation by Turbulence and Surfaces in Arbitrary Motion”, *Mathematical and Physical Sciences (1934-1990)*, Vol. 264 (1151), pp. 321-342, 1969.
- [2] F. Farassat, *Derivation of Formulations 1 and 1A of Farassat*, NASA/TM-2007-214853, 2007.
- [3] Alireza Najafi-Yazdi and Luc Mongeau, *An Acoustic Analogy Formulation for Uniformly Moving Media: Formulation 1C*, 16th AIAA/CEAS Aeroacoustics Conference, 2010. DOI: 10.2514/6.2010-3706
- [4] Choongmo Yang, Takashi Aoyama, Natsuki Kondo and Shigeru Saito. “Aerodynamic/Acoustic Analysis for Main Rotor and Tail Rotor of Helicopter”, *Trans. Japan Soc. Aero. Space Sci.*, Vol. 51, No. 171, pp. 28-36, 2008. DOI: 10.2322/tjsass.51.28
- [5] Y. Bu, W. Song, Z. Han, Y. Zhang, L. Zhang, “Aerodynamic/aeroacoustic variable-fidelity optimization of helicopter rotor based on hierarchical Kriging model”, *Chinese Journal of Aeronautics*, Vol. 33, Iss. 2, 2020, pp. 476-492. DOI: 10.1016/j.cja.2019.09.019
- [6] A. N. Kusyumov, S. A. Mikhailov, S. A. Kusyumov, K. V. Fayzullin, G. N. Barakos, “Numerical Simulation of Aeroacoustics of Hovering Helicopter Rotor”, *Materials Science and Engineering*, Vol. 449, 2018. DOI: 10.1088/1757-899X/449/1/012017
- [7] В. В. Пахова, К. В. Файзуллина, С. Л. Денисов, “Об измерении акустических характеристик модели несущего вертолетного винта в аэродинамической трубе”, *Акустический журнал*, том 66, № 1, с. 46-57, 2020.
- [8] R. Stepanov, V. Pakhov, A. Bozhenko, A. Batrakov, “Experimental and numerical study of rotor aeroacoustics”, *International Journal of Aeroacoustics*, Vol. 16, Iss. 6, pp. 460-475, 2017. DOI: 10.1177/1475472X1773044
- [9] Zhe Ning, Hui Hu, “An Experimental Study on the Aerodynamics and Aeroacoustic Characteristics of Small Propellers of UAV Applications”, 54th AIAA Aerospace Sciences Meeting, San Diego, California, USA, 2016. DOI: 10.2514/6.2016-1785

- [10] Nguyễn Hoàng Sơn, “Nghiên cứu tiếng ồn khí động trên máy bay trực thăng”, Luận văn thạc sĩ khoa học kỹ thuật cơ khí động lực, Đại học Bách khoa Hà Nội, 2019.
- [11] Phạm Thành Đồng, Nguyễn Anh Tuấn, Đặng Ngọc Thanh, Phạm Vũ Uy, “Xây dựng mô hình tính toán các đặc trưng khí động của cánh quay trực thăng”, *Tạp chí Khoa học và Kỹ thuật*, Số 185, 2017, tr. 70-79.
- [12] Phạm Thành Đồng, Lê Quang Quyền, Nguyễn Anh Tuấn, Vũ Quốc Trụ, “Nghiên cứu xác định đặc trưng tiếng ồn khí động của cánh quạt nâng trực thăng bằng phương pháp xoáy”, *Tuyển tập công trình Hội nghị khoa học các nhà nghiên cứu trẻ lần thứ XVII - năm 2022*, Học viện KTQS, 2022.
- [13] Q. Q. Le, T. D. Pham, A. T. Nguyen, Q. T. Vu, “Building and verifying a tool for calculating the aerodynamic noise of helicopter rotors”, *Journal of Science and Technique*, Vol. 17, No. 05, pp. 58-69, 2022. DOI: 10.56651/lqdtu.jst.v17.n05.530

## NGHIÊN CỨU ĐẶC TRƯNG TIẾNG ỒN KHÍ ĐỘNG CỦA CÁNH QUAY TRỰC THĂNG XÉT ĐẾN ẢNH HƯỞNG CỦA HÌNH DẠNG LÁ CÁNH

Lê Quang Quyền<sup>a</sup>, Phạm Thành Đồng<sup>a</sup>, Vũ Quốc Trụ<sup>a</sup>, Nguyễn Anh Tuấn<sup>a</sup>

<sup>a</sup>*Khoa Hàng không Vũ trụ, Trường Đại học Kỹ thuật Lê Quý Đôn*

**Tóm tắt:** Trong nghiên cứu này, các tác giả tiến hành khảo sát ảnh hưởng của hình dạng lá cánh đến đặc trưng tiếng ồn khí động của cánh quay trực thăng bằng phương pháp xoáy. Kết quả thu được là biến thiên hệ số lực nâng của cánh quay theo thời gian và đặc trưng tiếng ồn khí động của cánh quay trực thăng với một số hình dạng lá cánh khác nhau. Trên cơ sở đó đánh giá ảnh hưởng của hình dạng lá cánh đến các đặc trưng tiếng ồn khí động của cánh quay. Hình dạng lá cánh cải tiến được thiết kế nhằm giảm tiếng ồn khí động của cánh quay mà vẫn đảm bảo được giá trị lực nâng của cánh quay. Kết quả tính toán cho thấy rằng cánh quay với lá cánh cải tiến khi hoạt động tạo tiếng ồn nhỏ hơn và có thể giảm tới 6,15 dB (giảm 6,90%) so với cánh quay với lá cánh hình chữ nhật thông thường ở chế độ bay treo và giảm tới 5,4 dB (giảm 5,15%) ở chế độ bay bằng.

**Từ khóa:** *Phương pháp xoáy; cánh quay trực thăng; hình dạng lá cánh quay; tiếng ồn khí động.*

Received: 25/04/2023; Revised: 12/10/2023; Accepted for publication: 04/12/2023

